



Surface and bulk electronic structure of the strongly correlated system SmB_6 and implications for a topological Kondo insulator

N. Xu,^{1,*} X. Shi,^{1,2} P. K. Biswas,³ C. E. Matt,^{1,4} R. S. Dhaka,^{1,5} Y. Huang,¹ N. C. Plumb,¹ M. Radović,^{1,6} J. H. Dil,^{7,1} E. Pomjakushina,⁸ K. Conder,⁸ A. Amato,³ Z. Salman,³ D. McK. Paul,⁹ J. Mesot,^{1,5} H. Ding,² and M. Shi^{1,†}

¹Swiss Light Source, Paul Scherrer Institut, CH-5232 Villigen PSI, Switzerland

²Beijing National Laboratory for Condensed Matter Physics and Institute of Physics, Chinese Academy of Sciences, Beijing 100190, China

³Laboratory for Muon Spin Spectroscopy, Paul Scherrer Institut, CH-5232 Villigen PSI, Switzerland

⁴Laboratory for Solid State Physics, ETH Zürich, CH-8093 Zürich, Switzerland

⁵Institut de la Matière Complexe, EPF Lausanne, CH-1015, Lausanne, Switzerland

⁶SwissFEL, Paul Scherrer Institut, CH-5232 Villigen PSI, Switzerland

⁷Physik-Institut, Universität Zürich, Winterthurerstrass 190, CH-8057 Zürich, Switzerland

⁸Laboratory for Developments and Methods, Paul Scherrer Institut, CH-5232 Villigen PSI, Switzerland

⁹Physics Department, University of Warwick, Coventry CV4 7AL, United Kingdom

(Received 16 June 2013; published 10 September 2013)

Recent theoretical calculations and experimental results suggest that the strongly correlated material SmB_6 may be a realization of a topological Kondo insulator. We have performed an angle-resolved photoemission spectroscopy study on SmB_6 in order to elucidate elements of the electronic structure relevant to the possible occurrence of a topological Kondo insulator state. The obtained electronic structure in the whole three-dimensional momentum space reveals one electron-like $5d$ bulk band centered at the X point of the bulk Brillouin zone that is hybridized with strongly correlated f electrons, as well as the opening of a Kondo band gap ($\Delta_B \sim 20$ meV) at low temperature. In addition, we observe electron-like bands forming three Fermi surfaces at the center $\bar{\Gamma}$ point and boundary \bar{X} point of the surface Brillouin zone. These bands are not expected from calculations of the bulk electronic structure, and their observed dispersion characteristics are consistent with surface states. Our results suggest that the unusual low-temperature transport behavior of SmB_6 is likely to be related to the pronounced surface states sitting inside the band hybridization gap and/or the presence of a topological Kondo insulating state.

DOI: [10.1103/PhysRevB.88.121102](https://doi.org/10.1103/PhysRevB.88.121102)

PACS number(s): 73.20.-r, 71.20.-b, 75.70.Tj, 79.60.-i

A three-dimensional (3D) topological insulator (TI) is an unusual topological quantum state associated with unique metallic surface states that appear within the bulk band gap.^{1,2} Owing to the peculiar spin texture protected by time-reversal symmetry, the Dirac fermions in TIs are forbidden from scattering due to nonmagnetic impurities and disorder.^{3,4} Hence they carry dissipationless spin current,⁵ making it possible to explore fundamental physics, spintronics, and quantum computing.^{1,2} However, even after extensive materials synthesis efforts,⁶⁻¹⁰ impurities in the bulk of these materials make them metallic, prompting us to search for new types of TIs with truly insulating bulks.

The 3D Kondo insulator SmB_6 may open a new route to realizing topological surface states. SmB_6 is a typical heavy-fermion material with strong electron correlation. Localized f electrons hybridize with conduction electrons, leading to a narrow band gap on the order of 10 meV opening at low temperatures, with the chemical potential lying in the gap.¹¹⁻¹⁴ Due to the opening of the band gap, the conductivity changes from metallic to insulating behavior with decreasing temperature. It saturates to a constant value below about 1 K, which is thought to be caused by in-gap states.¹⁵ Theoretical studies have proposed that SmB_6 may host three-dimensional topological insulating phases.^{16,17} Recently, transport experiments employing a novel geometry^{18,19} showed convincing evidence of a distinct surface contribution to the conductivity that is unmixed with the bulk contribution, suggesting SmB_6 is an ideal topological insulator with a perfectly

insulating bulk. Point-contact spectroscopy revealed that the low-temperature Kondo insulating state harbors conduction states on the surface, in support of predictions of nontrivial topology in Kondo insulators.²⁰ Moreover, Lu *et al.* used the local-density approximation combined with the Gutzwiller method to investigate the topological physics of SmB_6 from the first principles.¹⁷ They found a nontrivial \mathbb{Z}_2 topology, indicating that SmB_6 is a strongly correlated topological insulator. They calculated the topological surface states and found three Dirac cones, in contrast to most known topological insulators. At present, topological insulators are essentially understood within the theory of noninteracting topological theory.^{1,2} SmB_6 , as one candidate for a topological Kondo insulator, potentially offers us an opportunity to investigate the interplay between topological states and strong many-body interactions.

As a surface-sensitive technique, angle-resolved photoemission spectroscopy (ARPES) is one of the best probes to investigate the surface states and attest to their topological nature. However, previous ARPES studies did not resolve the surface dispersion from bulk states, possibly due to the system resolution and sample surface condition.^{21,22} In this Rapid Communication, we report high-resolution ARPES results from SmB_6 in the whole three-dimensional Brillouin zone (BZ) by tuning the incident photon energy. Due to the high resolution of the ARPES system and good sample quality, we are able to clearly identify electron-like bands forming three Fermi surfaces (FS), which are distinct from the expected bulk

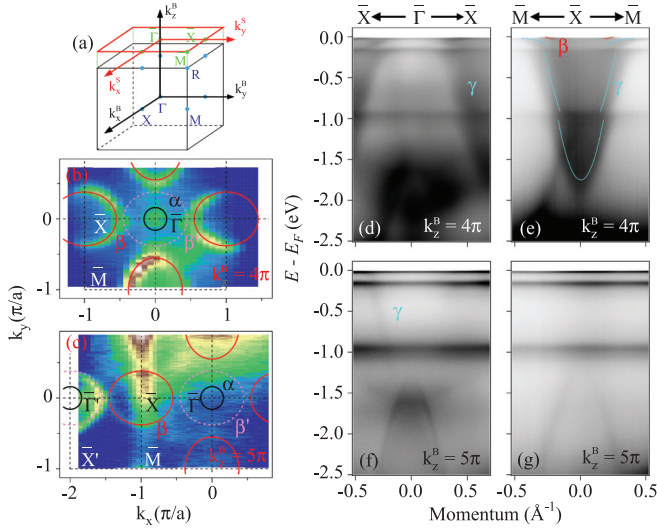


FIG. 1. (Color online) (a) The first Brillouin zone of SmB_6 and the projection on the cleaving surface. High-symmetry points are also indicated. (b), (c) Fermi surface mapping at $T = 17$ K by integrating ARPES intensity within $E_F \pm 5$ meV with $h\nu = 26$ and 46 eV, corresponding to $k_z^B = 4\pi$ and 5π at $\bar{\Gamma}$, respectively. (d), (e) ARPES intensity plots at $\bar{\Gamma}$ and \bar{X} for the $k_z^B = 4\pi$ plane at $T = 17$ K. The red and blue curves are the dispersions of the β and γ bands extracted by MDC fitting. (f), (g) Analogous to (d) and (e), but for the $k_z^B = 5\pi$ plane.

states, and we discuss the possible topological property of those surface states.

High-quality single crystals of SmB_6 were grown by the flux method. ARPES measurements were performed at the Surface/Interface Spectroscopy (SIS) beam line at the Swiss Light Source using a VG-Scienta R4000 electron analyzer with photon energies ranging from 22 to 110 eV. The energy resolution ranged from ~ 10 meV at 22 eV to ~ 15 meV at 110 eV. The angular resolution was around 0.2° . Clean surfaces for the ARPES measurements were obtained by cleaving the crystals *in situ* in a working vacuum better than 5×10^{-11} mbar. Shiny mirrorlike surfaces were obtained after cleaving the samples, confirming their high quality.

Figure 1 displays the Fermi surface and band dispersions of SmB_6 measured at $T = 17$ K with various photon energies, corresponding to different k_z points in the bulk BZ (k_z^B). The first BZ of bulk SmB_6 and its projection on the cleaving surface are shown in Fig. 1(a), with all the high-symmetry points labeled. In Figs. 1(b) and 1(c), we plot the FS mappings obtained using $h\nu = 26$ and 46 eV, allowing direct comparisons with previous work.^{21,22} In making the maps, we integrated the ARPES intensity within $E_F \pm 5$ meV. As seen in Figs. 1(b) and 1(c), the same FS topology is observed at different k_z^B high-symmetry points of the bulk BZ: one small circular FS, α , is located at the surface BZ center $\bar{\Gamma}$ point and an additional ellipse-shaped FS, β , is located at the surface BZ boundary \bar{X} point. We also observed a folded band β' caused by a 1×2 reconstruction of the surface, which is also observed in low-energy electron diffraction (LEED) patterns.²¹ Figures 1(d) and 1(e) show photoemission E vs k intensity plots at the $\bar{\Gamma}$ and \bar{X} points for the $k_z^B = 4\pi$ plane at $T = 17$ K.

Similarly, data recorded for the $k_z^B = 5\pi$ plane are shown in Figs. 1(f) and 1(g). One can see that the highly renormalized $4f^6$ electrons form three flat bands, located at $E_B = 960$, 160 , and 20 meV. One electron-like band, γ , hybridizes with three $4f^6$ bands at low temperature. The γ band, which is attributed to the $5d$ orbital as suggested by Ref. 17, is seen at \bar{X} for $k_z^B = 4\pi$ and at $\bar{\Gamma}$ for $k_z^B = 5\pi$, which in the bulk BZ are equivalent at the X point, as seen in Fig. 1(a). This strongly three-dimensional feature indicates that γ is a bulk band located at the X point in the bulk BZ, consistent with the theoretical calculation.¹⁷

In order to investigate the low-energy excitations, band dispersions near E_F at $\bar{\Gamma}$ and \bar{X} for the $k_z^B = 4\pi$ plane are shown in Figs. 2(a) and 2(b). In addition, we plot the ARPES intensity near E_F at the center of the second surface BZ $\bar{\Gamma}'$ point and \bar{X} point for the $k_z^B = 5\pi$ plane in Figs. 2(d) and 2(e). As seen in Figs. 2(b) and 2(d), the bulk band γ hybridizes with the flat $4f$ band near E_F , leading to a Kondo band gap. The gap size is $\Delta_B \sim 20$ meV based on the peak position of the energy distribution curve (EDC) taken at the position marked by the vertical red line in Fig. 2(b). Moreover, as

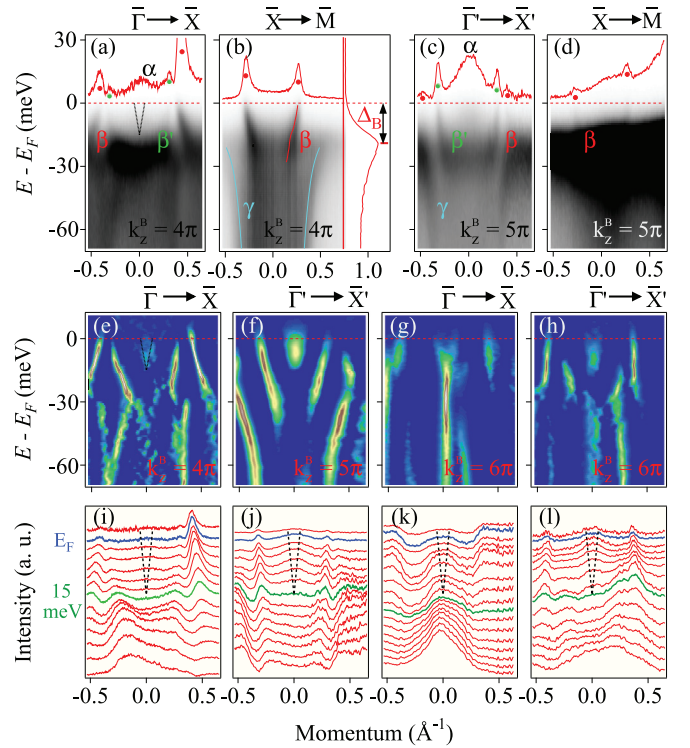


FIG. 2. (Color online) (a), (b) ARPES intensity plots for cuts through $\bar{\Gamma}-\bar{X}$ and $\bar{X}-\bar{M}$, respectively, for the $k_z^B = 4\pi$ plane. Note the narrow energy window. The data were collected at $T = 17$ K. The red and blue curves are dispersions for the β and γ bands extracted by fitting the MDCs. The curves on the top are the MDCs taken at E_F , with labels for the peak positions. An EDC at the location in k space marked by the red vertical line is also displayed. From this, the Kondo band gap is estimated to be $\Delta_B \sim 20$ meV. (c), (d) Analogous to (a) and (b), but for the $k_z^B = 5\pi$ plane. (e)–(g) Plots of the curvatures of the MDC intensities along $\bar{\Gamma}-\bar{X}$ in either the first or second BZ ($\bar{\Gamma}'-\bar{X}'$) evaluated in the $k_z^B = 4\pi$, 5π , and 6π planes, respectively. (h) MDC curvature analysis at the second BZ center $\bar{\Gamma}'$ point for the $k_z^B = 6\pi$ plane. (i)–(l) Corresponding MDC plots for (e)–(h).

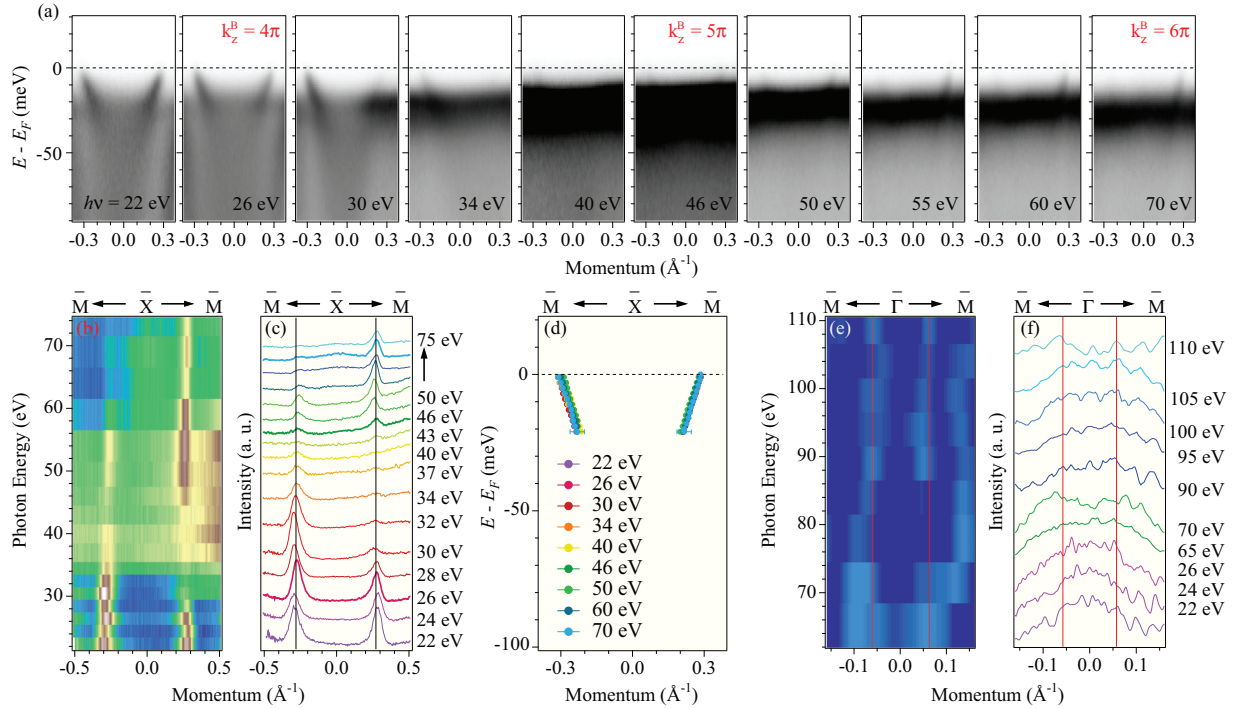


FIG. 3. (Color online) (a) ARPES intensity along the \bar{X} - \bar{M} direction measured at $T = 17$ K with various photon energies. (b) Plot of the ARPES intensity along \bar{X} - \bar{M} as a function of photon energies from 22 to 75 eV, covering more than 1.5 BZs along k_z^B . (c) Corresponding MDCs at E_F . (d) Extracted dispersions of the β band for different photon energies. (e) Plot of the curvature of the MDC intensity along $\bar{\Gamma}$ - \bar{M} for each photon energy. (f) Corresponding MDCs at E_F .

seen in Figs. 2(b) and 2(d), the electron-like band β appears inside the band gap and crosses E_F at the \bar{X} point, forming an ellipse-shaped FS at the BZ boundary. For the β band, its Fermi momentum k_F measures 0.39 and 0.28 \AA^{-1} along the \bar{X} - $\bar{\Gamma}$ and \bar{X} - \bar{M} directions, respectively. The folded band β' can be seen in Figs. 2(a) and 2(c), located at about $\bar{\Gamma}$, with a folding wave vector $(\pi, 0)$ caused by the 1×2 surface reconstruction. Additionally, we observe one weak band α at the $\bar{\Gamma}$ point, which corresponds to the small FS at the BZ center. To better visualize the weak α band, in Figs. 2(e)–2(h) we plot the curvature of the MDC intensity²³ along $\bar{\Gamma}$ - \bar{M} for different photon energies approximately corresponding to the $k_z^B = 4\pi, 5\pi$, and 6π planes. The corresponding raw momentum distribution curves (MDCs) are also plotted in Figs. 2(i)–2(l). From the curvature plots, we can see that the electron-like α band crosses E_F around the $\bar{\Gamma}$ point, which can also be observed in the MDC plots. The MDCs at E_F in Figs. 2(a) and 2(c) confirm that the α and β bands indeed cross E_F .

From bulk band calculations,^{16,17} the in-gap bands α and β are totally unexpected at any k_z^B value. However, both theoretical and experimental results^{16–18,20} suggest that SmB_6 exhibits metallic surface states that make it a candidate for a strongly correlated Kondo topological insulator. To further examine whether the in-gap states are surface or bulk bands, we have carried out an ARPES measurement along the cut crossing the \bar{X} point for different k_z^B values by tuning photon energy. In Fig. 3(a) we plot ARPES spectra with k_{\parallel} oriented along the \bar{X} - \bar{M} line taken with different photon energies from 22 to 70 eV, which cover more than 1.5 bulk BZs along

k_z^B . One can see that, although the spectral weight of the β band varies with photon energy due to photoemission matrix element effects, the dispersion of the β band stays highly fixed. MDCs at E_F obtained with different photon energies are plotted in Fig. 3(c), and the corresponding $h\nu$ - k_{\parallel} FS intensity plot is shown in Fig. 3(b). As one immediately recognizes from Fig. 3(c), the peak positions of the MDCs at E_F , which indicate the k_F values of the β band, are stationary with respect to $h\nu$. Thus the β band forms a two-dimensional FS in the $h\nu$ - k_{\parallel} plane shown in Fig. 3(b). In fact, when we plot the extracted dispersions for different photon energies in Fig. 3(d), their linear dispersions overlap each other within the experimental uncertainties, demonstrating the two-dimensional nature of the β band. This two-dimensional feature is different from the bulk γ band, indicating the surface origin of the β band. We likewise studied the photon energy dependence of the small α band to check its surface/bulk origin. While the weak intensity and shallow dispersion make detailed quantitative analysis of the α band difficult, we consistently find anomalous spectral weight at E_F connected to this band, independent of the photon energy. This is consistent with a shallow 2D state that is nondispersive along k_z . In light of the fact that the α band is not predicted from bulk band structure calculations, the data strongly suggest that the α band, like the β band, has a surface origin.

We have also performed temperature-dependent measurements to study the evolution of both the bulk and surface bands. Figures 4(a)–4(f) show ARPES intensity plots at the \bar{X} point measured at temperatures ranging from 17 to 280 K. Figures 4(g)–4(i) show similar plots at the $\bar{\Gamma}$ point measured

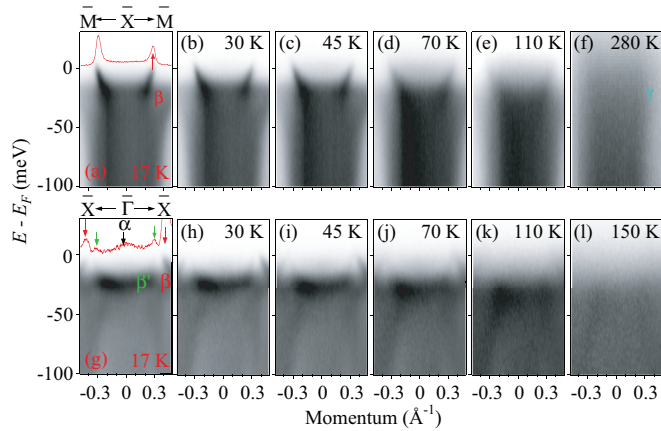


FIG. 4. (Color online) (a)–(f) ARPES intensity plots along \bar{M} – \bar{X} – \bar{M} measured at $T = 17, 30, 45, 70, 110,$ and 280 K, respectively. (g)–(l) ARPES intensity plots along \bar{X} – $\bar{\Gamma}$ – \bar{X} measured at $T = 17, 30, 45, 70, 110,$ and 150 K, respectively.

at temperatures ranging from 17 to 150 K. The hybridization between the $5d$ γ band and $4f$ flat band is destroyed around $T = 110$ K. Meanwhile, the surface bands α and β , as well as the folding band β' , vanish. The temperature dependence suggests that the surface states can only exist when the Kondo band gap opens.

Our ARPES results demonstrate that SmB_6 is a strongly correlated Kondo insulator with metallic surface states located inside the Kondo band gap. The observed surface bands at both the $\bar{\Gamma}$ and \bar{X} points show good agreement with the topologically nontrivial surface states found in calculations,¹⁷ suggesting that SmB_6 is a topological Kondo insulator as predicted theoretically.^{16,17} Three surface bands (α contributes one FS at the $\bar{\Gamma}$ point and β contributes two FSs at the \bar{X} point) enclose an odd number of time-reversal-invariant momenta, which is a very strong indication of a topologically nontrivial phase. We also note that no clear Dirac point is observed in our ARPES measurements; for the α band, the intensity is too dim to see a potential Dirac point clearly. One possible reason is that the cleaving surface is the B-terminated layer, and the α band may originate from Sm, making the signal

very weak. For the β band, the intensity diminishes suddenly at $E_B \sim 20$ meV, corresponding to the hybridization gap edge between f and d electrons, which may prohibit observing the Dirac point formed by the bands crossing each other. Thus the apparent absence of a clear Dirac point may be a signature of interactions between topological surface states and the strongly correlated bulk f electrons. Such nontrivial many-body interactions have recently been observed in other topological insulators studied by ARPES.²⁴ This hints that SmB_6 may offer an opportunity to understand topological insulators beyond the noninteracting topological theory. It should also be mentioned that the identified surface states in our ARPES experiments are robust. As a test, after acquiring ARPES data from a fresh surface right after cleaving at low temperature (18 K), we have warmed the sample to room temperature and placed the sample in 5×10^{-8} mbar for 48 h. After cooling down to 18 K, the surface states were still clearly visible.

In summary, we reported high-resolution ARPES results from the strongly correlated Kondo insulator SmB_6 . We first identified two anomalous bands, α located at the BZ center $\bar{\Gamma}$ and β at the BZ boundary \bar{X} , that are distinct from the expected bulk band structure. While the shallow dispersion of the α band prevents clear analysis of its shape as a function of k_z , we managed to explicitly show that the β band is a 2D surface state. The observation of these states agrees well with the topologically nontrivial surface states predicted by theoretical calculations.^{16,17} We also observe that the α and β bands disappear when the hybridization between the bulk γ band and the heavily correlated f electrons vanishes at high temperature. Our results uphold the possibility that SmB_6 is a topological Kondo insulator, consistent with theoretical calculations.^{16,17}

We acknowledge Z. Fang for stimulating discussions. This work was supported by the Sino-Swiss Science and Technology Cooperation (Project No. IZLCZ2138954), the Swiss National Science Foundation (Grant No. 200021-137783), and MOST (Grant No. 2010CB923000) and NSFC. The experiment was carried out at the Swiss Light Source of the Paul Scherrer Institut in Villigen, Switzerland, and we thank the SIS beam line staff for their excellent support.

*nan.xu@psi.ch

†ming.shi@psi.ch

¹M. Z. Hasan and C. L. Kane, *Rev. Mod. Phys.* **82**, 3045 (2010).

²X. L. Qi and S. C. Zhang, *Rev. Mod. Phys.* **83**, 1057 (2011).

³Y. Xia, D. Qian, D. Hsieh, L. Wray, A. Pal, H. Lin, A. Bansil, D. Grauer, Y. S. Hor, R. J. Cava, and M. Z. Hasan, *Nat. Phys.* **5**, 398 (2009).

⁴S. Souma, K. Kosaka, T. Sato, M. Komatsu, A. Takayama, T. Takahashi, M. Kriener, K. Segawa, and Y. Ando, *Phys. Rev. Lett.* **106**, 216803 (2011).

⁵C. L. Kane and E. J. Mele, *Science* **314**, 1692 (2006).

⁶H. Peng, K. Lai, D. Kong, S. Meister, Y. Chen, X. Qi, S. Zhang, Z. Shen, and Y. Cui, *Nat. Mater.* **9**, 225 (2010).

⁷J. G. Checkelsky, Y. S. Hor, R. J. Cava, and N. P. Ong, *Phys. Rev. Lett.* **106**, 196801 (2011).

⁸J. G. Analytis, R. D. McDonald, S. C. Riggs, J. Chu, G. S. Boebinger, and I. R. Fisher, *Nat. Phys.* **6**, 960 (2010).

⁹A. A. Taskin and Y. Ando, *Phys. Rev. B* **80**, 085303 (2009).

¹⁰D. Kim, S. Cho, N. P. Butch, P. Syers, K. Kirshenbaum, S. Adam, J. Paglione, and M. S. Fuhrer, *Nat. Phys.* **8**, 460 (2012).

¹¹P. Coleman, in *Handbook of Magnetism and Advanced Magnetic Materials* (Wiley, New York, 2007), Vol. 1, p. 95.

¹²G. Aeppli and Z. Fisk, *Comments Condens. Matter Phys.* **16**, 155 (1992).

- ¹³H. Tsunetsugu, M. Sigrist, and K. Ueda, *Rev. Mod. Phys.* **69**, 809 (1997).
- ¹⁴P. Riseborough, *Adv. Phys.* **49**, 257 (2000).
- ¹⁵A. Menth, E. Buehler, and T. H. Geballe, *Phys. Rev. Lett.* **22**, 295 (1969).
- ¹⁶M. Dzero, K. Sun, V. Galitski, and P. Coleman, *Phys. Rev. Lett.* **104**, 106408 (2010).
- ¹⁷F. Lu, J. Z. Zhao, H. Weng, Z. Fang, and X. Dai, *Phys. Rev. Lett.* **110**, 096401 (2013).
- ¹⁸D. J. Kim, S. Thomas, T. Grant, J. Botimer, Z. Fisk, and J. Xia, arXiv: 1211.6769.
- ¹⁹S. Wolgast, C. Kurdak, K. Sun, J. W. Allen, D. Kim, and Z. Fisk, arXiv: 1211.5104.
- ²⁰X. H. Zhang, N. P. Butch, P. Syers, S. Ziemak, R. L. Greene, and J. Paglione, *Phys. Rev. X* **3**, 011011 (2013).
- ²¹H. Miyazaki, T. Hajiri, T. Ito, S. Kunii, and S. I. Kimura, *Phys. Rev. B* **86**, 075105 (2012).
- ²²S. K. Mo, G. H. Gweon, J. D. Denlinger, H. D. Kim, J. W. Allen, C. G. Olson, H. Hochst, J. L. Sarrao, and Z. Fisk, *Phys. B* **281–282**, 716 (2000).
- ²³P. Zhang, P. Richard, T. Qian, Y.-M. Xu, X. Dai, and H. Ding, *Rev. Sci. Instrum.* **82**, 043712 (2011).
- ²⁴T. Kondo, Y. Nakashima, Y. Ota, Y. Ishida, W. Malaeb, K. Okazaki, S. Shin, M. Kriener, S. Sasaki, K. Segawa, and Y. Ando, *Phys. Rev. Lett.* **110**, 217601 (2013).